A Phase Diagram for the Binary Blends of Nearly Symmetric Diblock Copolymers. 2. Parameter Space of Temperature and Blend Composition†

Daisuke Yamaguchi, Hirokazu Hasegawa, and Takeji Hashimoto*

Department of Polymer Chemistry, Graduate School of Engineering, Kyoto University, Kyoto 606-8501, Japan

Received December 18, 2000; Revised Manuscript Received May 25, 2001

ABSTRACT: A phase diagram in the parameter space of temperature and blend composition that contains order−disorder transition (ODT) and thermoreversible macrophase separation between constituent copolymers was constructed for binary blends of polystyrene-*block*-polyisoprene (PS−PI) copolymers. The constituent copolymers, designated as H102 and FS-1, have nearly symmetric copolymer compositions and rather different molecular weights; i.e., number-average molecular weight (M_n) and volume fraction of PS-block (f_{PS}) are 1.0×10^5 and 0.47 for H102 while 2.1×10^4 and 0.40 for FS-1. The ODT was observed on the neat FS-1 and two blend specimens whose weight fractions of H102, Φ_{H102}, are 0.1 and 0.2. Counterintuitively, the ODT temperature (T_{ODT}) decreased with increasing the average molecular weight of the specimen, namely, T_{ODT} for FS-1 neat > T_{ODT} for the blend of $\Phi_{H102} = 0.1$ > T_{ODT} for the blend of $\Phi_{H102} = 0.2$. Then T_{ODT} abruptly increased between the blends of $\Phi_{H102} = 0.2$ and 0.3 and became inaccessibly high temperature (i.e., > 200 °C). The macrophase separation between H102 and FS-1 was observed on the blend of $\Phi_{H102} = 0.2$. This macrophase separation was thermoreversible but accompanied by a hysteresis between cooling and heating processes. Although both H102 and FS-1 neat copolymers showed lamellar morphology, PS cylindrical morphology was observed on certain blend specimens. The origin of PS cylindrical morphology may be attributed to the slight asymmetry in the f_{PS} of FS-1.

I. Introduction

Block copolymers provide fascinating research topics, due to their variety of properties, including the order−disorder transition (ODT), the order−order transition (OOT), and the wide variety of morphologies in the ordered state.[1,2] Recently, the blends of two different block copolymers, such as $(A-B)_\alpha/(A-B)_\beta$ where A−B denotes A-*block*-B copolymer, also have received considerable theoretical[3−9] and experimental[10−29] attention due to their richness of the phase behaviors, including macrophase separation,[8,9,13−15,23,27] microphase separation,[10,11,16−26,29] macrophase separation induced by microphase separation,[14] OOT,[4,5,19−21,24,26] and modulated or superlattice structures.[15]

In the previous study,[30] we investigated the interplay of macro- and microphase transitions by employing binary mixtures of polystyrene (PS)-*block*-polyisoprene (PI) (PS−PI) diblock copolymers which have similar molecular weights but different compositions, namely, the volume fractions of PS-block (f_{PS}). On the other hand, in this paper we focus on the binary mixtures of PS−PI having similar compositions; i.e., the f_{PS} of each copolymer is close to 0.5 but rather different molecular weights.

As for the $(A-B)_\alpha/(A-B)_\beta$ blends, in which both copolymers have similar compositions but different molecular weights, many experimental and theoretical studies have been reported previously.[4,6,8,10,12−14,18,22,23,27] One of the important problems of those mixtures is controlling the properties of block copolymers, such as the size of microdomain and the ODT temperature (T_{ODT}), by changing the blend composition.

In the earlier works, Hadziioannou and Skoulios investigated the change of structural parameters of lamellar microdomains such as the lamellar spacing and the interfacial area per junction of block copolymer, with changing the blend composition of binary mixtures of block copolymers, each of which is di- or triblock copolymer composed of PS and PI with $f_{PS} \approx 0.5$ and hence has lamellar morphology.[10] Later, Lin et al.[22] and Kane et al.[23] investigated the dependence of domain spacing as a function of the blend composition for the miscible blends of nearly symmetric PS−PI copolymers and found some new aspects. On the theoretical side, some groups explored the relation between the structural properties and chain organization for the system that contains polydisperse polymer chains.[4,6,8]

The ODT of blends of block copolymers has been also investigated by some research groups. Almdal et al. investigated the ODT of binary blends of nearly symmetric poly(ethylenepropylene)-*block*-poly(ethylethylene) (PEP−PEE) copolymers using rheological methods and found that the temperature range of ODT for binary blends was relatively broader than that for pure copolymers,[12] while Bodycomb et al.[17] and Floudas et al.[18] observed a sharp ODT for the binary blends of nearly symmetric PS−PI copolymers by using small-angle X-ray scattering (SAXS) and rheological methods, respectively. The discrepancy between these two observations seems to be due to the difference in the characteristics of the blend specimens employed in these studies, as will be described later in section IV.2.

The miscibility criteria for the molecular weight difference between $(A-B)_\alpha$ and $(A-B)_\beta$ and the complicated self-assembled structures involving the macrophase separation between $(A-B)_\alpha$ and $(A-B)_\beta$ and the microphase separation of A and B block are also important problems. This problem was experimentally

† Presented in part at the 47th Symposium of the Society of Polymer Science, Japan, Oct 1998. *Polym. Prepr. Jpn., Soc. Polym. Sci., Jpn.* **1998**, *47*, 2684−2685.

* To whom correspondence should be addressed.

10.1021/ma0021491 CCC: $20.00
Published on Web 08/01/2001

explored by Hashimoto et al.[13] They investigated the miscibility criterion for the binary blend of PS−PI copolymers, each of which is nearly symmetric and forms lamellar morphology. The result of the work[13] is that, in the case of the molecular weight ratio (r) is smaller than about 5, the two constituent copolymers are miscible on the molecular level and form the single ordered microdomain morphology, while in the case of $r > 10$, the two constituent copolymers phase-separate each other and each phase forms its own microdomain morphology.[13] The theoretical exploration of this problem has been done by Matsen in the context of self-consistent-field theory (SCFT).[8] The calculation result of ref 8 is consistent with the earlier experimental study by Hashimoto et al.[13] and further confirmed other experimental studies by Kane et al.,[23] Papadakis et al.,[27] and part 1 of this series.[31]

However, all the previous experimental studies concerning the miscibility and morphology of binary blends of A−B diblock copolymers having the nearly same block compositions $f_{A,\alpha} \cong f_{A,\beta} \cong f_A \cong 0.5$ have been carried out under a given temperature T (e.g., the ambient temperature) as a function of r and blend composition Φ_α. To the best of our knowledge, the phase transition from a miscible state to an immiscible state induced by changing temperature has not been reported up to now. Our objective in this paper is to report the experimental observation of the thermoreversible phase transition between a miscible state at high temperatures and an immiscible state at low temperatures for a binary mixture of PS−PI diblock copolymers, which have $f_{PS} \cong 0.5$ for the both block copolymers but rather different molecular weights. Note that the present study, concerning a phase diagram of $(A-B)_\alpha/(A-B)_\beta$ blends having $f_A \cong 0.5$ and having a particular value of $r \cong 4.8$ in the parameter space of T and Φ_α, can be regarded as being complementary to a companion paper of the phase diagram in the parameter space of r and Φ_α at a given T on the same blend systems.[31] In the parameter space of T and Φ_α as well, we find the cylindrical phase, which is intriguing because both component block copolymers by themselves form lamellar phase. However, the physical origin of the cylinder should be referred to the companion paper.[31]

II. Experimental Section

II.1. Sample Preparation. Two nearly symmetric and lamellar-forming PS−PI's used in this study were synthesized by living anionic polymerization with *sec*-butyllithium as an initiator and cyclohexane as a solvent. While in this study the long and short copolymers are coded as H102 and FS-1, respectively, they are identical to α and β_4 employed in the companion paper,[31] respectively. Therefore, here we describe only number-average molecular weight (M_n), molecular weight distribution (M_w/M_n), and volume fraction of PS block (f_{PS}) of these copolymers: H102 has $M_n = 1.0 \times 10^5$, $M_w/M_n = 1.16$, and $f_{PS} = 0.47$[31,32] while FS-1 has $M_n = 2.1 \times 10^4$, $M_w/M_n = 1.04$, and $f_{PS} = 0.40$.[31] Sample characterization was done by GPC. In each synthesis a precursory PS sample was taken out before the second step polymerization of PI to determine the molecular weight of the PS block by GPC. GPC was calibrated not only for PS standard homopolymers but also for PI standard homopolymers to determine correctly the molecular weight of both PS and PI block. The volume fraction of PS (f_{PS}) characterized by GPC showed a good agreement with that characterized by ^{1}H NMR. Film specimens were cast from a 5 wt % polymer in toluene solution. 0.5 wt % of antioxidant (Irganox 1010, Ciba-Geigy Group) was added to the film specimens in the casting process to prevent the thermal degradation of the specimens during the following measurements. The blend specimens with different blend compositions were prepared and are designated as (H102/FS-1) 10/90, 20/80, 30/70, 40/60, and 70/30 to denote the weight ratio of the larger diblock copolymer to the smaller diblock copolymer.

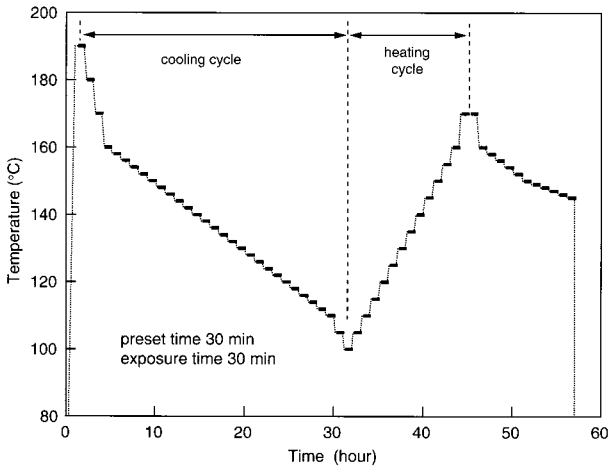

Figure 1. Typical thermal program given in the SAXS experiments. For neat FS-1 and blend samples, whose weight fractions of H102 are 0.1, 0.2, and 0.3, measurements were first conducted on cooling process and then followed by heating process as presented here. At each temperature, the specimen was held for 30 min before the measurement (broken line), and the measurement lasted for 30 min (thick line).

II.2. Small-Angle X-ray Scattering. For each neat diblock copolymer and blend specimen, temperature-dependent small-angle X-ray scattering (SAXS) was measured in situ with a SAXS apparatus described elsewhere, except for the replacement of the X-ray generator with a new one (MAC Sciences M18X HF operated at 18 kW).[33−35] All measurements were conducted with specimens placed under nitrogen atmosphere to reduce thermal degradation. The typical thermal protocol employed in the SAXS experiments is shown in Figure 1. Namely, the as-cast specimen was initially elevated to the highest measured temperature and held at that temperature for about an hour to erase the memory built up in the casting process. Then the first run of measurement at each temperature was conducted during the cooling process, and the second run of measurement at each temperature was conducted during the heating process to examine the thermoreversibility. At each temperature, the specimen was held for 30 min before the measurement and the measurement lasted for 30 min. SAXS profiles were desmeared for slit width and slit height smearing and corrected for air scattering, absorption, and thermal diffuse scattering.[33−35] The absolute intensity was obtained by the nickel-foil method.[36]

II.3. Transmission Electron Microscopy. Microphase- or macrophase-separated morphologies of the specimens were observed by transmission electron microscopy (TEM). For TEM observation, the film specimens were microtomed at −100 °C, using a Reichert Ultracut E low-temperature sectioning system. The ultrathin sections were stained with the vapor of 2% OsO_4(aq) for a few hours.[37] TEM observation was done with a Hitachi H-600S transmission electron microscope operated at 75 kV and in the bright field mode. The thermal protocols of the specimens used for TEM observations are listed in Table 1.

III. Results

III.1. Neat Diblock Copolymers. Figure 2, shows the SAXS profiles taken at ambient temperature for the neat diblock copolymers, H102 and FS-1, where q is the magnitude of scattering vector defined by $q = (4\pi/\lambda)\sin(\theta/2)$ with λ and θ being the wavelength of X-ray and scattering angle, respectively. In each profile the higher-order scattering maxima locate at the positions of integer multiples relative to the position of the first-

Table 1. Thermal Protocols for TEM Specimens

sample code	Figure No.	thermal history[a]
FS-1	3b	a.t. → 180 °C (1 h) → 178 °C (1 h) → 176 °C (1 h) → 174 °C (1 h) → 172 °C (1 h) → 170 °C (1 h) → 165 °C (1 h) → 160 °C (1 h) → 155 °C (1 h) → 150 °C (1 h) → 145 °C (1 h) → 140 °C (1 h) → 135 °C (1 h) → 130 °C (1 h) → 120 °C (1 h) → 110 °C (1 h) → 100 °C (1 h) → 90 °C (1 h) → 80 °C (1 h) →70 °C (1 h) → a.t.
10/90	8	a.t. → 190 °C (1 h) → 180 °C (1 h) → 170 °C (1 h) → 168 °C (1 h) → 164 °C (1 h) → 162 °C (1 h) → 160 °C (1 h) → 158 °C (1 h) → 156 °C (1 h) → 154 °C (1 h) → 152 °C (1 h) → 150 °C (1 h) → 145 °C (1 h) → 140 °C (1 h) → 130 °C (1 h) → 120 °C (1 h) → 110 °C (1 h) → 100 °C (1 h) → 90 °C (1 h) → 80 °C (1 h) → 70 °C (1 h) → a.t.
20/80 (I)	13a	a.t. → 190 °C (1 h) → 180 °C (1 h) → 170 °C (1 h) → 165 °C (1 h) → 160 °C (1 h) → 159 °C (1 h) → 158 °C (1 h) → 157 °C (1 h) → 156 °C (1 h) → 155 °C (3 h) → 0 °C (ice water)
20/80 (II)	13b	a.t. → 190 °C (1 h) → 180 °C (1 h) → 170 °C (1 h) → 160 °C (1 h) → 155 °C (1 h) → 150 °C (1 h) → 149 °C (1 h) → 148 °C (1 h) → 147 °C (1 h) → 146 °C (1 h) → 145 °C (3 h) → 0 °C (ice water)
20/80 (III)	13c	a.t. → 190 °C (1 h) → 180 °C (1 h) → 170 °C (1 h) → 160 °C (1 h) → 155 °C (1 h) → 150 °C (1 h) → 148 °C (1 h) → 146 °C (1 h) → 144 °C (1 h) → 142 °C (1 h) → 140 °C (1 h) → 138 °C (1 h) → 136 °C (1 h) → 134 °C (1 h) → 132 °C (1 h) → 130 °C (1 h) → 128 °C (1 h) → 126 °C (1 h) → 124 °C (1 h) → 122 °C (1 h) → 120 °C (1 h) → 115 °C (1 h) → 110 °C (1 h) → 100 °C (1 h) → 90 °C (1 h) → 80 °C (1 h) → 70 °C (1 h) → a.t.
30/70	18a	a.t. → 200 °C (1 h) → 190 °C (1 h) → 180 °C (1 h) → 170 °C (1 h) → 160 °C (1 h) → 150 °C (1 h) → 145 °C (1 h) → 140 °C (1 h) → 135 °C (1 h) → 130 °C (1 h) → 125 °C (1 h) → 120 °C (1 h) → 115 °C (1 h) → 110 °C (1 h) → 100 °C (1 h) → 90 °C (1 h) → 80 °C (1 h) → 70 °C (1 h) → a.t.
40/60	18b	a.t. → 200 °C (1 h) → 190 °C (1 h) → 185 °C (1 h) → 180 °C (1 h) → 175 °C (1 h) → 170 °C (1 h) → 165 °C (1 h) → 160 °C (1 h) → 155 °C (1 h) → 150 °C (1 h) → 145 °C (1 h) → 140 °C (1 h) → 135 °C (1 h) → 130 °C (1 h) → 125 °C (1 h) → 120 °C (1 h) → 110 °C (1 h) → 100 °C (1 h) → 90 °C (1 h) → 80 °C (1 h) → 70 °C (1 h) → a.t.
70/30	19b	a.t. → 110 °C (12 h) → 100 °C (1 h) → 90 °C (1 h) → 80 °C (1 h) → 70 °C (1 h) → a.t.
H102	3a	a.t. → 110 °C (12 h) → 100 °C (1 h) → 90 °C (1 h) → 80 °C (1 h) → 70 °C (1 h) → a.t.

[a] The number inside parentheses denotes the holding period at that temperature, and a.t. means the ambient temperature.

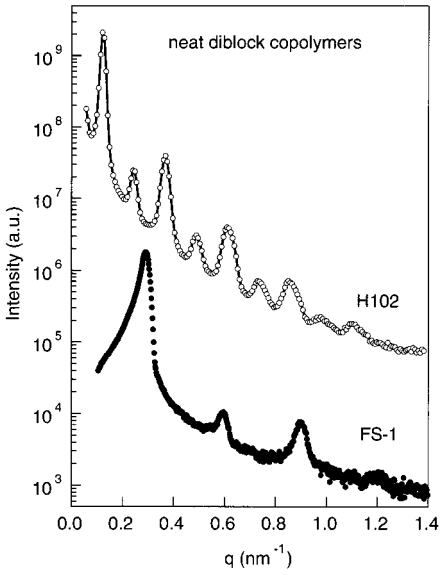

Figure 2. SAXS profiles for neat diblock copolymers, H102 and FS-1, taken at ambient temperature.

order scattering maximum, indicating that alternating lamellar microdomains of PS and PI are formed. The second-order peak is small compared with the third-order peak, suggesting that the volume fraction of PS domains is close to 0.5 for each specimen. This is consistent with the fact that both H102 and FS-1 have nearly symmetric compositions. Further, the magnitude of the scattering vector for the first-order scattering maximum (q_m) of H102 is much smaller than that of FS-1, indicating that the domain spacing of H102 is larger than that of FS-1. Figure 3 shows the TEM micrographs of (a) H102 neat and (b) FS-1 neat. We discern that the both neat diblock copolymers form lamellar morphology, and the lamellar thickness of H102 is thicker than that of FS-1, in good agreement with the SAXS results shown in Figure 2.

The larger copolymer, H102, retains lamellar morphology over the temperature range from ambient temperature to 200 °C due to its relatively high molecular weight, whereas the smaller copolymer, FS-1, shows a sharp ODT in the temperature range investigated here. Figure 4 shows the SAXS profiles from neat

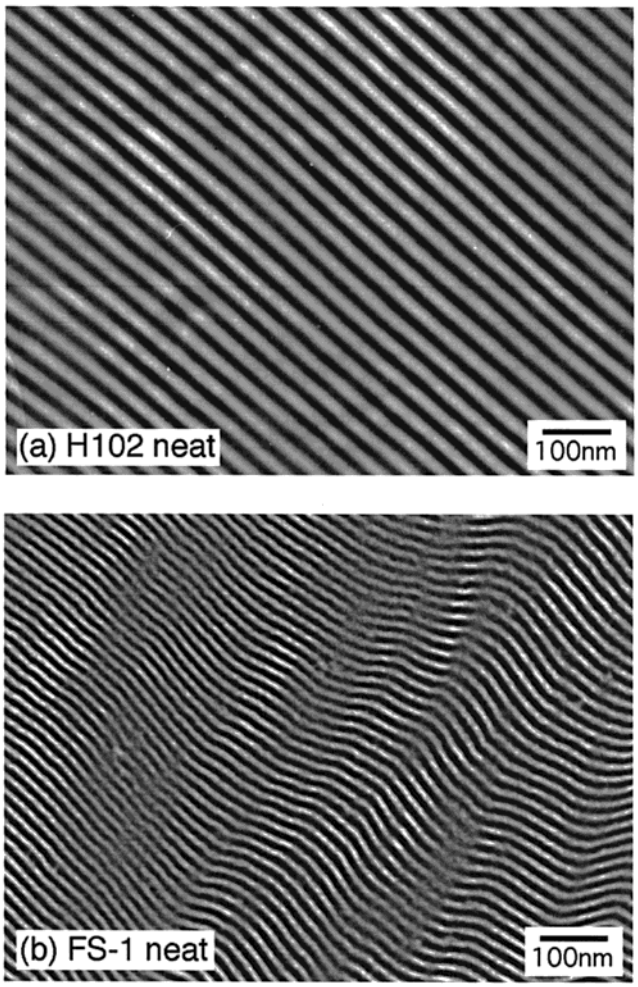

Figure 3. TEM micrographs of neat diblock copolymers, H102 (part a) and FS-1 (part b).

FS-1 taken at various temperatures during the cooling process. A sharp and remarkable change of the profiles is clearly discerned at temperatures between 172 and 174 °C. To characterize the change in the SAXS profile across the ODT, Figure 5 shows (a) I_m^{-1}, (b) σ_q^2, and (c)

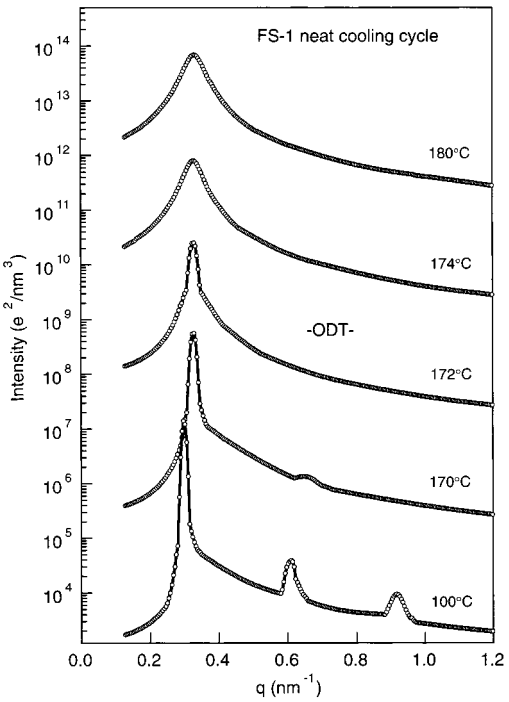

Figure 4. Desmeared SAXS profiles of FS-1 neat copolymer taken at various temperatures on cooling process. Each curve is shifted up by a factor of 10^2 relative to the unshifted curve at 100 °C to avoid overlap. We found an abrupt change on the profile, which is regarded as a sign of ODT, occurred between 174 and 172 °C.

D plotted as a function of reciprocal absolute temperature, T^{-1}, where I_m^{-1}, σ_q^2, and D denote the reciprocal of peak scattered intensity (I_m), the square of the half-width at half-maximum of the scattering peak (σ_q), and the characteristic length obtained by $D = 2\pi/q_m$, respectively. As expected, both I_m^{-1} and σ_q^2 show a sharp discontinuous change in the temperature range between 170 and 175 °C. Thus, for neat FS-1 copolymer, we determined the ODT temperature based on the cooling process, $T_{ODT} = 173 \pm 1$ °C.

III.2. Blend Specimens. *H102/FS-1 = 10/90 Blend.* Figure 6 shows the SAXS profiles of H102/FS-1 = 10/90 taken at various temperatures during the cooling process from 190 °C. We discern that a sharp and remarkable profile change occurs at temperatures between 158 and 162 °C. Since this profile change, namely, an abrupt sharpening and increasing of I_m, is very similar to that observed on the ODT of FS-1 neat copolymer, we assess it as the ODT of H102/FS-1 = 10/90 blend. To characterize the change in the SAXS profile along the ODT of H102/FS-1 = 10/90, we plot (a) I_m^{-1}, (b) σ_q^2, and (c) D as a function of T^{-1} in Figure 7. From Figure 7a,b, we discern the abrupt change of I_m^{-1} and σ_q^2 in the temperature range between 158 and 165 °C. Moreover, for the 10/90 blend, we discern D decreases discontinuously at the temperatures between 160 and 162 °C with increasing T^{-1}. Note that this discontinuous change in D is not observed in the case of neat block copolymer, FS-1 (see Figure 5c). With further decreasing temperature below the T_{ODT}, the higher-order scattering peaks appear on the SAXS profiles of the 10/90 blend as presented in Figure 6, which suggests formation of the lamellar morphology with a long-range order.

The lamellar morphology for the 10/90 blend is also confirmed by TEM observation as shown in Figure 8. Thus, as for the H102/FS-1 = 10/90 blend, we concluded

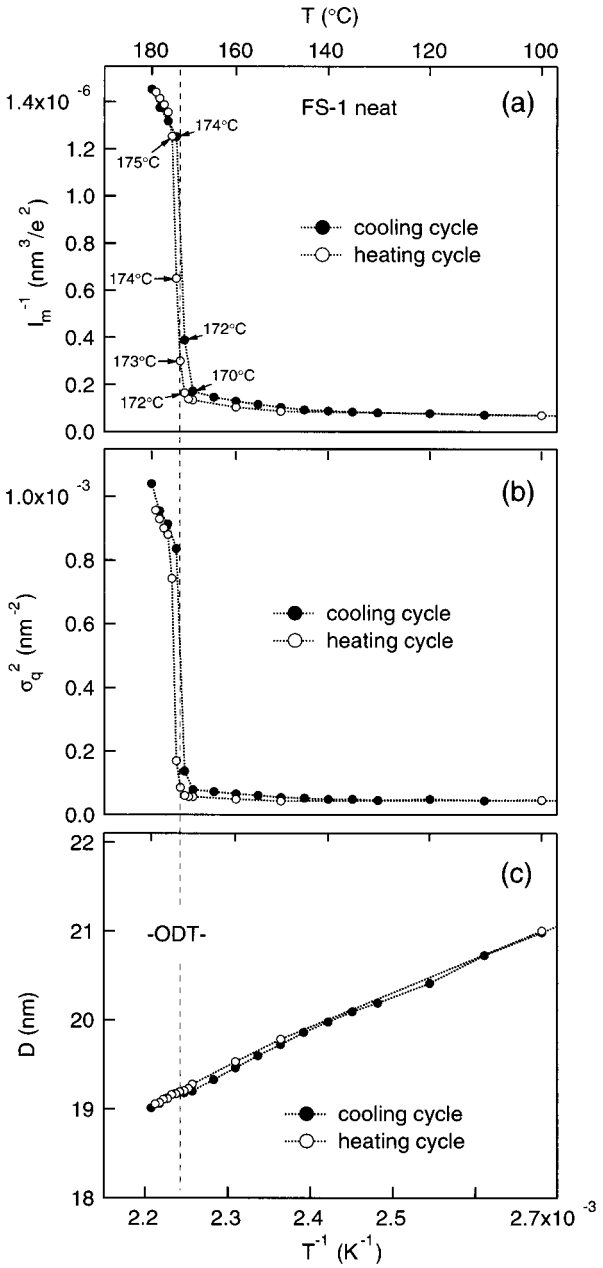

Figure 5. Plots of I_m^{-1} (part a), σ_q^2 (part b), and D (part c) vs T^{-1} for FS-1 neat copolymer. In these plots, filled circle (●) and open circle (○) denote the values measured on cooling and heating processes, respectively.

that an ordinary ODT from the disordered state to the ordered state of lamellar morphology takes place at $T_{ODT} = 161 \pm 1$ °C, which is determined on the basis of the cooling process.

H102/FS-1 = 20/80 Blend. For the H102/FS-1 = 20/80 blend the phase behavior with changing temperature is rather complicated. Figure 9a,b shows the SAXS profiles of the 20/80 taken at various temperatures during the cooling process from 200 °C. Further, to observe the change on the SAXS profile in detail, parts a−c and parts d−f of Figure 10 highlight the temperature dependence of the first-order scattering peak during cooling process and heating process, respectively. It should be noted that all of the profiles shown in Figure 10 were not subjected to the correction for slit width and slit height smearing to avoid any artifacts involved by the desmearing process.

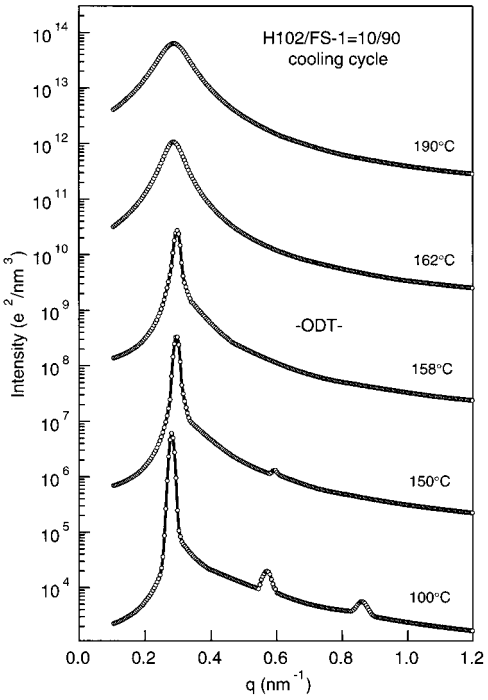

Figure 6. Desmeared SAXS profiles of H102/FS-1 = 10/90 blend taken at various temperatures on cooling process. Each curve is shifted up by a factor of 10^2 relative to the unshifted curve at 100 °C to avoid overlap. We found that an abrupt change on the profile, which is regarded as a sign of ODT, occurred between 162 and 158 °C.

At 200 °C, as shown in Figure 9a, the SXAS profile of the 20/80 blend has a single broad scattering maximum typical of the disordered state. As the temperature decreased from 200 °C, the scattering peak increased in intensity and sharpened continuously until 150 °C, and then a discontinuous change occurred at temperatures between 150 and 148 °C as shown in Figure 10a. This discontinuous change in peak intensity, breadth, and position is very similar to the ODT behavior observed in the 10/90 blend. Thus, we assessed this discontinuous behavior as the ODT of the 20/80 blend and determined the T_{ODT} in the cooling process at 149 ± 1 °C. A further decrease of temperature below the T_{ODT} for the 20/80 blend induced the ordering of the system and led to the further intensity increasing and sharpening of the first-order peak. However, as presented in Figure 9, even at 140 °C there were no distinct higher-order scattering maxima or shoulders on the SAXS profile of the 20/80 blend. However, below 140 °C, a change other than evolution of the higher-order scattering maxima eventually took place.

As shown in Figure 10b, below 140 °C the first-order scattering peak began to decrease in intensity, broaden, and shift to the smaller q with decreasing temperature, and finally, at 134 °C two additional shoulders, which are marked by arrow in Figure 10b, were discerned together with the first-order peak. Upon further decreasing T toward 120 °C (Figure 10c), on one hand the original first-order peak became weaker and disappeared; on the other hand, the two scattering maxima that are first discerned at 134 °C as shoulders increased and sharpened, resulting in two main peaks at 120 °C, suggesting that a macrophase transition occurred in this temperature range. Here the macrophase transition means the transition from the state in which H102 and FS-1 are totally miscible on the molecular level and form

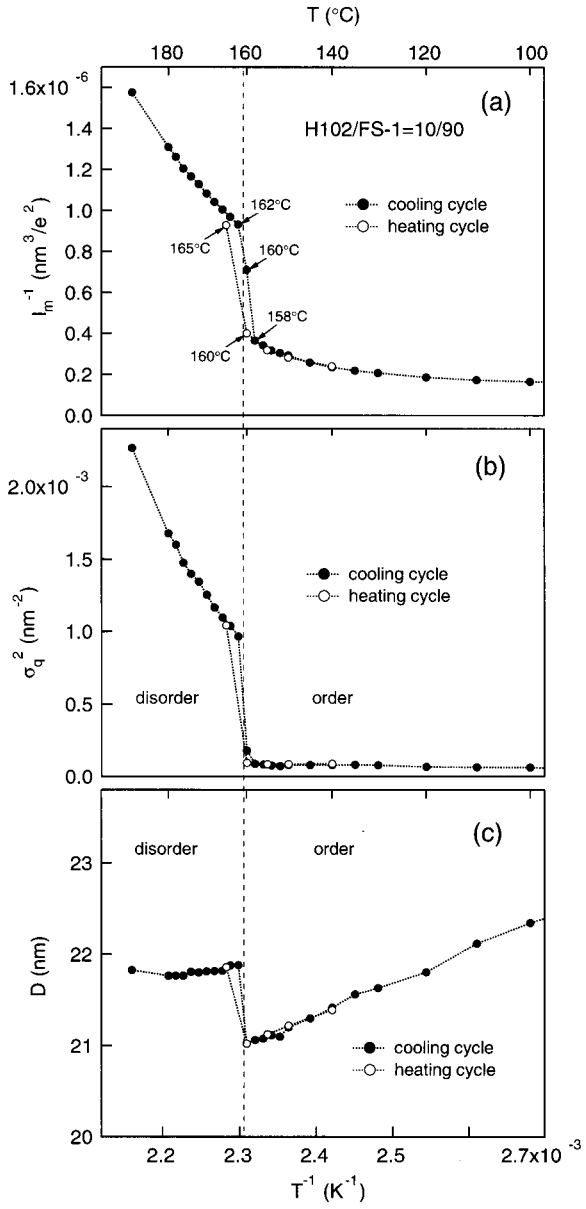

Figure 7. Plots of I_m^{-1} (part a), σ_q^2 (part b), and D (part c) vs T^{-1} for H102/FS-1 = 10/90 blend. In these plots, filled circle (●) and open circle (○) denote the values measured on cooling and heating processes, respectively.

a single ordered phase to the state in which H102 and FS-1 are only partially miscible and form macroscopically phase-separated, two coexisting ordered phases.

After the macrophase transition occurred, the ordering of each phase proceeded with decreasing temperature, and the respective higher-order scattering maxima became discerned on the SAXS profile. For example, we can find four clear scattering maxima on the SAXS profile of the 20/80 blend taken at 100 °C as shown in Figure 9b. The first and second peaks, indicated respectively by the arrow with number 1 and by the arrow with number 1 in the box, correspond to the first-order scattering peaks originated from H102-rich and FS-1-rich phases, respectively, and the third and fourth peaks, indicated by the arrows with numbers 2 and 3 in the box, which locate at the positions of twice and thrice as large as the position of second-order peak, respectively, indicate the second- and third-order scattering peak originated from the FS-1-rich phase. Fur-

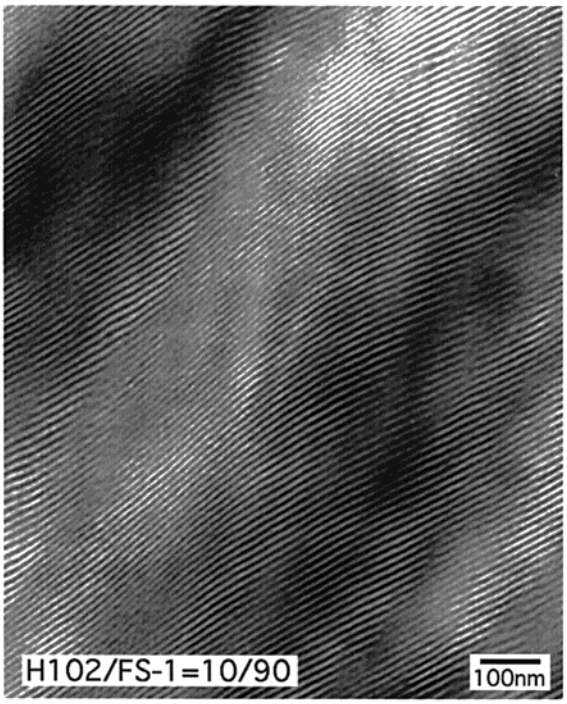

Figure 8. TEM micrograph of the H102/FS-1 = 10/90 blend.

thermore, there is a broad and small shoulder between the first-order and second-order peaks of the FS-1-rich phase. This shoulder locates at around the position of $\sqrt{3}$ relative to that of the first-order peak of H102-rich phase, suggesting that the morphology of the H102-rich phase has a hexagonal symmetry.

Thus, we can summarize the phase behavior of the 20/80 blend on the cooling process as follows: (i) In the temperature range from 200 to 150 °C, the two constituent copolymers, H102 and FS-1, are totally miscible on the molecular level in the disordered state. We hereafter refer to this stage as state I for the sake of convenience. (ii) An ODT takes place at $T_{ODT} = 149 \pm 1$ °C, and the two constituent copolymers are totally miscible on the molecular level and form a single ordered structure with a particular periodicity at temperatures between 148 and 140 °C. This stage is hereafter referred to state II. (iii) Below 138 °C constituent copolymers becomes partially miscible, and the ordered structure begins to separate into two macrophase-separated coexisting phases with different periodicities. We hereafter refer to this stage as state III. The various states observed in the cooling process are summarized in Figure 11a for convenience. Note here that one interesting problem concerning this macrophase separation is the mechanism of the separation, namely whether the separation occurs via spinodal decomposition or nucleation and growth. However, it seems very hard to make a clear discussion about the mechanism with the data we have shown here. This issue is beyond the scope of this study and deserves a future work.

A further complication arose in that the scattering behavior of the 20/80 blend on the heating process is different from that on the cooling process. As shown in Figure 10d,e, the two first-order scattering peaks originated from the H102-rich and FS-1-rich phases were clearly discerned up to 140 °C, and then these two peaks began to merge into a single peak with further increasing temperature. However, as shown in Figure 10f, even at 150 °C the scattering profile with one main peak and one shoulder marked by arrows suggested the sign of macrophase separation, and further increasing temperature up to 155 °C led to the direct transition to the state I without passing through the state II, as summarized in Figure 11b.

To characterize this highly complicated SAXS behavior for the 20/80 blend, we show I_m^{-1}, σ_q^2, and D plotted as a function of T^{-1} in parts a−c of Figure 12. In Figure 12, the filled and open symbols denote the values measured on cooling and heating processes, respectively, and the assignments of states I, II, and III are determined from the behavior of cooling process. It should be noted that in Figure 12 the values of I_m^{-1}, σ_q^2, and D were obtained from desmeared SAXS profiles[38] shown in Figure 9. From Figure 12, we notice that at temperatures above 155 °C in state I or below 125 °C in state III, the behaviors of I_m^{-1}, σ_q^2, and D on heating process and cooling process are almost identical, whereas at temperatures between 130 and 150 °C they are quite different. Such a hysteresis between heating and cooling process is not observed in the ODT of FS-1 neat copolymer or the 10/90 blend and may be originated from the metastable character of state II. We will discuss about this issue later in the section IV.4.

To confirm the complex phase behavior of the 20/80 blend suggested by SAXS measurement, the real space observation by TEM was conducted. The three specimens representative of state I, II, and III were prepared for TEM observation, and the details of their thermal protocols are summarized in Table 1. Generally speaking, the TEM observations and the SAXS behaviors are in agreement as will be described below. Figure 13a shows the TEM micrograph of the 20/80 blend quenched from 155 °C, at which the specimen is in state I according to the SAXS measurement. In Figure 13a, the PS and PI microdomains, which appear bright and dark, respectively, are distributed rather randomly and that the system can be looked upon as in the disordered state having the fluctuation-induced disordered structure (D_F).[39] Figure 13b shows the TEM micrograph of the 20/80 blend quenched from 145 °C, at which the specimen is in state II according to the SAXS measurement. In Figure 13b the sample space is filled with the grains composed of the ordered lamellar microdomains with single periodicity.[40]

Figure 13c shows TEM micrograph of the 20/80 blend gradually cooled to the ambient temperature whose scattering profile corresponds to that of 100 °C shown in Figure 9b. On the basis of the SAXS profile, we can interpret Figure 13c as follows. In this specimen the constituent copolymers, H102 and FS-1, are only partially miscible, and they form macroscopically phase-separated structures in which microdomains with different domain spacings and morphologies coexist: one, which appears to be lamellar morphology with a smaller domain spacing and occupies the major part of the sample space, and the other, which appears to be cylindrical morphology with a larger domain spacing and whose grains are located on upper and lower side of the central part of Figure 13c. Of course, the former and latter are expected to correspond to FS-1-rich and H102-rich phases, respectively. Note that, as for the H102-rich phase, the TEM image clearly shows that it has nonlamellar morphology. Although an unequivocal determination of its morphology is difficult from this TEM image alone, we tend to interpret, from the TEM

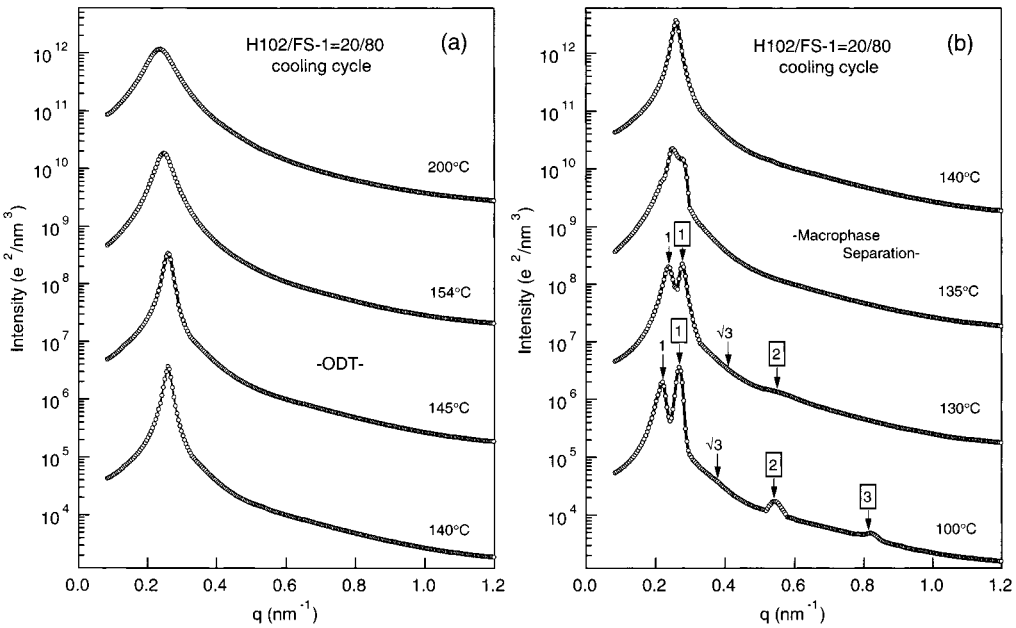

Figure 9. Desmeared SAXS profiles of the H102/FS-1 = 20/80 blend taken at various temperatures between 200 and 140 °C (part a) and below 140 °C (part b) on cooling process. Each curve is shifted up by a factor of 10^2 relative to the unshifted curve at 140 (a) and 100 °C (b) to avoid overlap. We found that in (a) a discontinuous sharpening of scattering maximum that is regarded as a sign of ODT occurred between 154 and 145 °C. In addition, we noticed that in (b) a splitting of principal scattering maximum that is considered as a sign of macrophase separation started from 135 °C.

image and the SAXS profiles in Figure 9b, that the H102-rich phase likely has a hexagonally packed PS cylinder. Therefore, hereafter we just tentatively assign PS cylindrical morphology to the H102-rich phase in the 20/80 blend, and this does not mean to completely rule out the possibility of another kind of bicontinuous morphology.

H102/FS-1 = 30/70 and 40/60 blends. In Figures 14 and 15, we show the SAXS profiles of H102/FS-1 = 30/70 and 40/60, respectively, taken at various temperatures during the cooling process from 200 °C. There are two similarities between the phase behavior of the 30/70 blend and that of the 40/60 blend. First of all, both 30/70 and 40/60 blends retain ordered state up to 200 °C and hence do not show the ODT in the range between ambient temperature and 200 °C. I_m^{-1} and σ_q^2 plots for the first-order peak for the 30/70 and 40/60 blends, which are shown in parts a and b of Figures16 and 17, respectively, show almost no change with changing T^{-1}, confirming that these blends do not have the ODT in this temperature range. The other similarity between these two blends is concerned with the morphology. Both the SAXS profile of the 30/70 blend taken at 150 °C and that of the 40/60 blend taken at 200 °C show higher-order scattering maxima at the positions of $\sqrt{3}$ and 2 relative to the position of first-order scattering maximum, suggesting the cylindrical morphology.

The two blends, however, show the following dissimilarity. In the case of 30/70 blend, lowering temperature produced an extra scattering maximum, which is discerned on the SAXS profiles below 120 °C and marked with an asterisk in Figure 14, at the position of ~1.39 relative to the position of the first-order scattering peak. As for this scattering peak, we can consider two interpretations. One is that this scattering peak corresponds to one of the higher-order scattering maxima of the first-order peak and a morphological transition from cylinder to another complicated bicontinuous structure takes place at a temperature between 150 and 120 °C. The other possibility is that this scattering peak corresponds to the first-order scattering peak of the FS-1-rich phase, and the other three scattering peaks, which are still retained at 150 °C, are originated from the coexisting hexagonal cylinder phase in the H102-rich phase. Namely, a phase transition from the state, in which H102 and FS-1 are totally miscible on the molecular level and form a single ordered phase, to the state, in which H102 and FS-1 are only partially miscible and form two-coexisting ordered phases, takes place at a temperature between 150 and 120 °C. These two possibilities are screened by TEM observation. The 40/60 blend, however, exhibits no tendency for the macrophase separation.

To check the morphologies of the 30/70 and the 40/60 blends, we conducted the real space observation by TEM. The details of the thermal protocols for these specimens are summarized in Table 1. Figure 18b, which shows the TEM image of the 40/60 blend, suggests that the whole sample space of the 40/60 blend is filled uniformly with the PS cylindrical morphology. This image corresponds to that obtained in the section in which the cylindrical axes orient nearly normal to it. These observations are in good agreement with the SAXS results of the 40/60 blend as shown in Figure 15. On the other hand, from Figure 18a, which shows the TEM image of the 30/70 blend, we can discern that there are two coexisting ordered phases in the sample space: one seems to be PS cylindrical morphology with a larger domain spacing and is located on the right upper side of the image, and the other seems to be lamellar morphology with a smaller domain spacing and is located on the left upper side of the image. This macrophase-separated morphology of the 30/70 blend is similar to that of the 20/80 blend, shown in Figure 13c. Moreover, as for the SAXS profiles, we can find the similarity between the 30/70 blend and the 20/80 blend. On the SAXS profiles of the 30/70 blend taken at 120 or 100 °C, shown in Figure 14, the first-order peak and

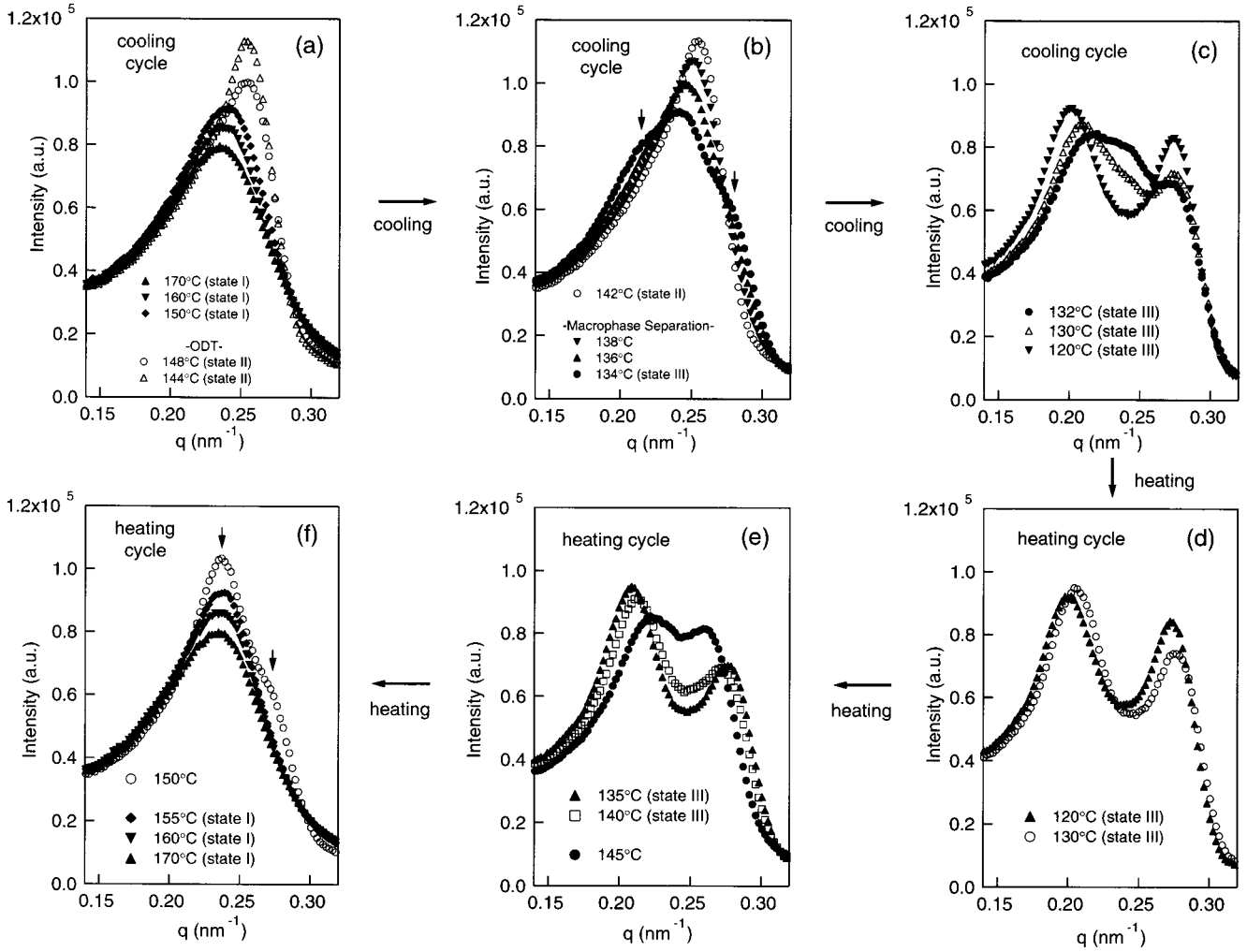

Figure 10. Highlight of the main scattering maximum on the smeared SAXS profiles of H102/FS-1 = 20/80 blend taken at various temperatures on both cooling (a−c) and heating (d−f) processes. To prevent any artifacts induced by slit corrections, the profiles without slit corrections are presented here.

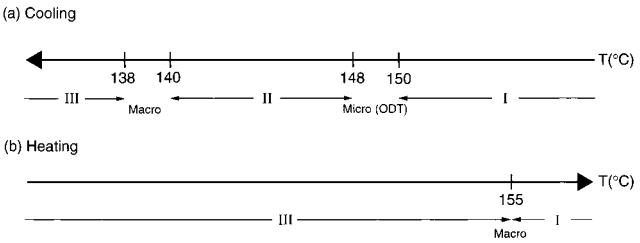

Figure 11. Various states of $(PS-PI)_\alpha/(PS-PI)_\beta$ observed in the cooling (a) and heating processes (b). States I to III refer to disordered single phase, ordered single phase, and ordered two-phase, respectively. Micro and macro denotes microphase (order−disorder) transition and macrophase transition.

the peak designated with the asterisk are located at the positions of $q = 0.20-0.22$ nm^{-1} and $q = 0.28-0.29$ nm^{-1}, respectively, while on the SAXS profiles of the 20/80 blend taken at 130 or 100 °C, shown in Figure 9b, the first-order peaks of H102-rich and FS-1-rich phases are located at the positions of $q = 0.22-0.23$ nm^{-1} and $q = 0.27-0.28$ nm^{-1}, respectively. Therefore, judging from the similarities in the peak positions, we concluded that the scattering peak designated with the asterisk in Figure 14 corresponds to the first-order scattering maximum originated from FS-1-rich phase forming the lamellar morphology. Concerning the morphology of H102-rich phase of the 30/70 blend, judging from both TEM image and SAXS profile, whose higher-order scattering maxima are located at the positions of $\sqrt{3}$ and 2 relative to the position of first-order scattering peak, we considered it as PS cylindrical morphology.

Another different point between the 30/70 and 40/60 blends is the temperature dependence of D, shown in Figures 16c and 17c, respectively. From these plots we discern that for the 40/60 blend D monotonically increases with T^{-1}, which is similar to the behavior of D observed on the FS-1 neat copolymer as shown in Figure 5c, whereas for the 30/70 blend D first gradually decreases with T^{-1} in the single-phase region and then splits into values in the two-phase region: the spacing having larger D increases with T^{-1}, while that having smaller D does not change with T^{-1}. However, a through investigation for the origin of this unusual behavior of D is beyond the scope of this paper and will not be discussed further.

H102/FS-1 = 70/30 Blend. Figure 19 shows (a) the SAXS profile and (b) the TEM micrograph of the 70/30 blend. As for the 70/30 blend, we could not determine the T_{ODT} because it is too high and out of the measurement range (i.e., >200 °C) and just checked its morphology. The thermal protocols of the specimens for SAXS and TEM are identical and described in Table 1. The SAXS profile was taken at ambient temperature. Both

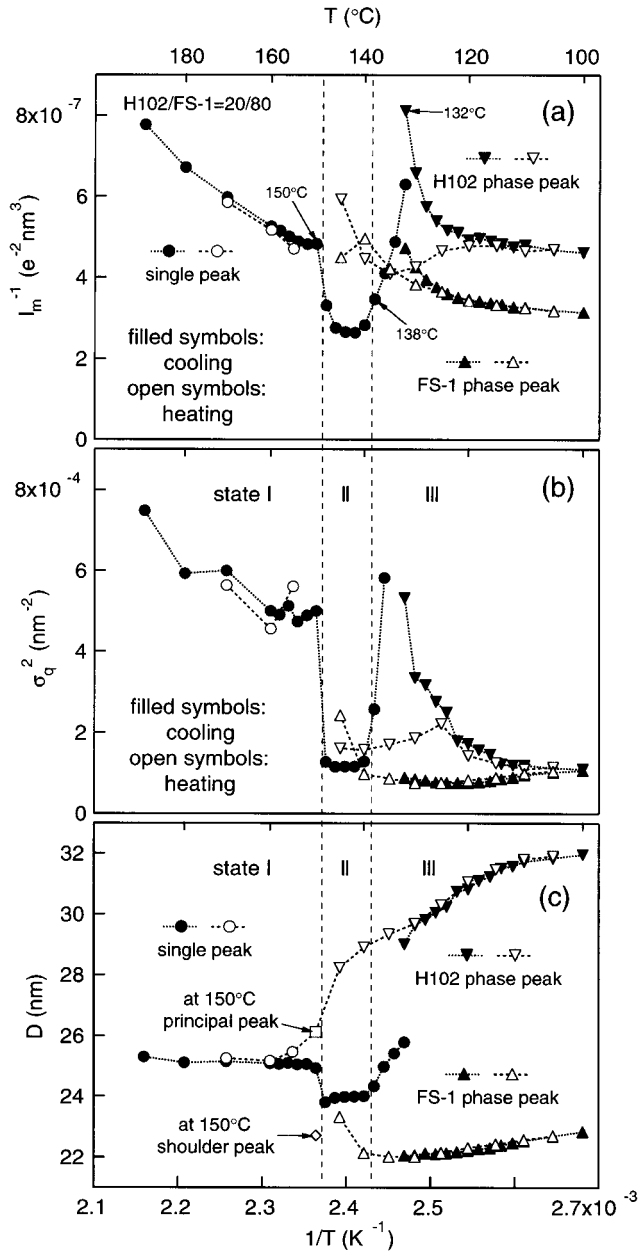

Figure 12. Plots of I_m^{-1} (a), σ_q^2 (b), and D (c) vs T^{-1} for the H102/FS-1 = 20/80 blend. In these plots, the open and filled symbols denote the values measured on cooling and heating processes, respectively. In these plots, the values from the single phase region are denoted by circles (●, ○), and the values from the peaks located at smaller- and wider-angle in the two-phase region are denoted by upset triangles (▼, ▽) and triangles (▲, △), respectively.

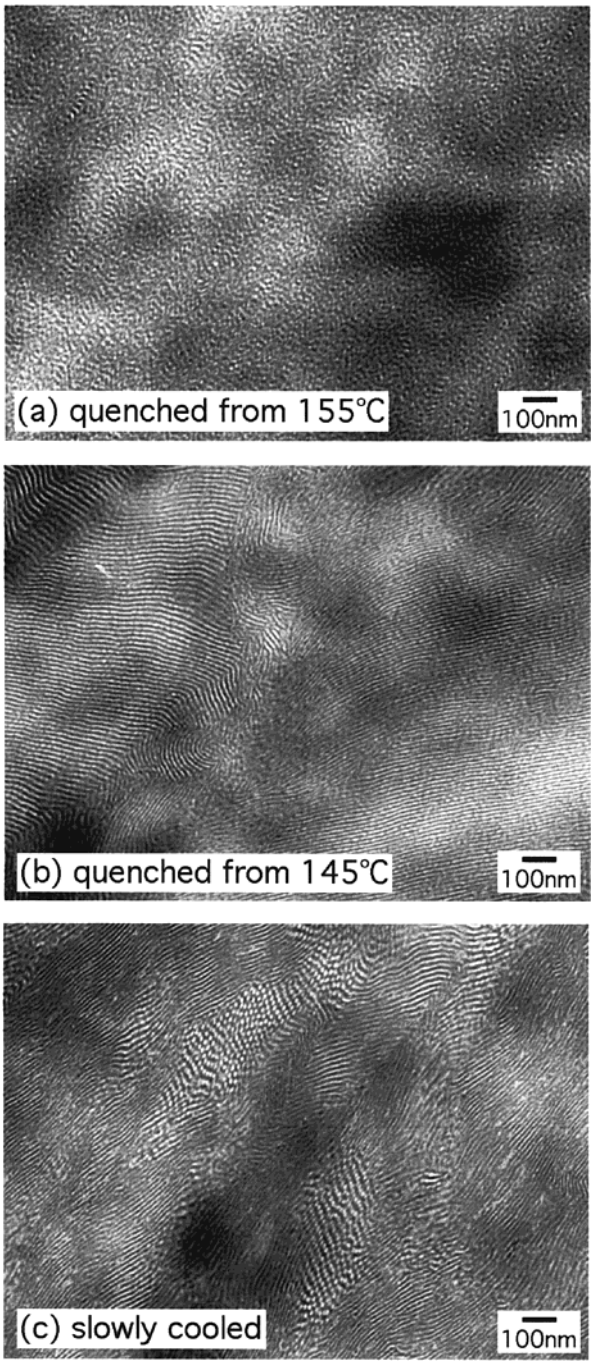

Figure 13. TEM micrographs of the H102/FS-1 = 20/80 blend taken from the specimens quenched from 155 (a) or 145 °C (b) into ice water and slowly cooled from 200 °C to ambient temperature. Further details of thermal protocols for those specimens are summarized in Table 1.

the SAXS and TEM results clearly show that the 70/30 blend possesses lamellar morphology.

IV. Discussion

IV.1. Phase Diagram. In Figure 20, we summarize the phase diagram of H102/FS-1 blends based on the SAXS measurements on cooling process. Let us survey this phase diagram briefly and pick up the remarkable features to facilitate the following discussions. First, as for ODT, we have observed ODT for the specimens, whose weight fractions of H102 (hereafter designated as Φ_{H102}) range from 0 to 0.2. It is interesting to note that T_{ODT} is the highest for neat short copolymer, FS-1, and T_{ODT} decreases with adding the longer copolymer, H102. Second, for the blends of $0.2 \leq \Phi_{H102} \leq 0.3$, we have observed the partial miscibility of H102 and FS-1 and macroscopically phase-separated, coexisting two ordered phases. Third, we observe the interesting hysteresis between heating and cooling processes on the blend of $\Phi_{H102} = 0.2$ (see Figures 10−12), although in Figure 20 we show only the results on the cooling process and that hysteresis is not presented. As for the morphology, we have observed interestingly enough PS cylindrical morphology on the blends of $0.2 \leq \Phi_{H102} \leq 0.4$. However, since this topic is intensively discussed in the companion study,[31] we shall not repeat the discussion here.

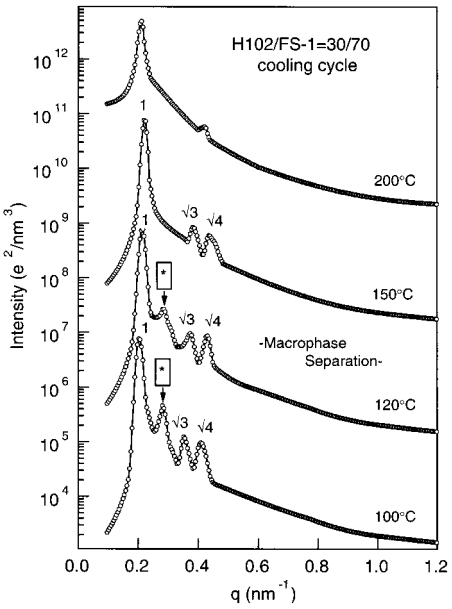

Figure 14. Desmeared SAXS profiles of the H102/FS-1 = 30/70 blend taken at various temperatures on cooling process. Each curve is shifted up by a factor of 10^2 relative to the unshifted curve at 100 °C to avoid overlap. We found the peak marked with an asterisk to infer the existence of different phase from that corresponds to the other three peaks located at 1, $\sqrt{3}$, and $\sqrt{4}$ relative to the position of the first-order peak, at temperatures below 120 °C.

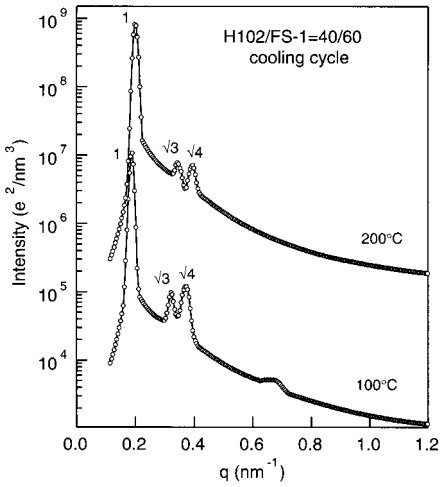

Figure 15. Desmeared SAXS profiles of the H102/FS-1 = 40/60 blend taken at 200 and 100 °C. The curve taken at 200 °C is shifted up by a factor of 10^2 relative to the other to avoid overlap. Both profiles are typical of the cylindrical morphology.

IV.2. Order−Disorder Transition. It is worthy to note that previously Almdal et al.[12] and Floudas et al.[18] independently investigated the ODT of the binary mixtures of the symmetric diblock copolymers by rheology. In both cases, the T_{ODT}'s of the blend specimens were determined from the discontinuity in the plots of G' vs T measured at a sufficiently low frequency. In the case of ref 18, two symmetric PS−PI block copolymers with similar polymerization indices (r = 1.35) are employed. The T_{ODT} which was characterized by sharp discontinuity in G' increased with increasing the amount of the large molecular weight block copolymer or increasing the number-average degree of polymerization N_n,[18] while in the case of ref 12, two symmetric PEP−PEE copolymers with r = 2.58 are employed. The sharp discontinuity of the transition in the plots of G' vs T is lost for the blend specimens, and the ODT seems to occur continuously over the temperature range of ca. 15 °C.[12] However, the tendency that the ODT increases with increasing of the mass-average degree of polymerization of the blend specimen is retained.[12] Thus, the tendency observed on H102/FS-1 blends with a large value of r = 4.8 that T_{ODT} decreases with increasing Φ_{H102} is contrary to what previous studies[12,18] reported. As for the origin of decrease of T_{ODT} with increasing Φ_{H102}, we cannot help but consider as follows. The small fraction of the large molecular weight block copolymer of H102 incorporated into the lamellae composed of FS-1 enhances the instability of lamellar packing. This instability of lamellar packing causes the decrease of T_{ODT} for the blend specimens. In fact, a further increase

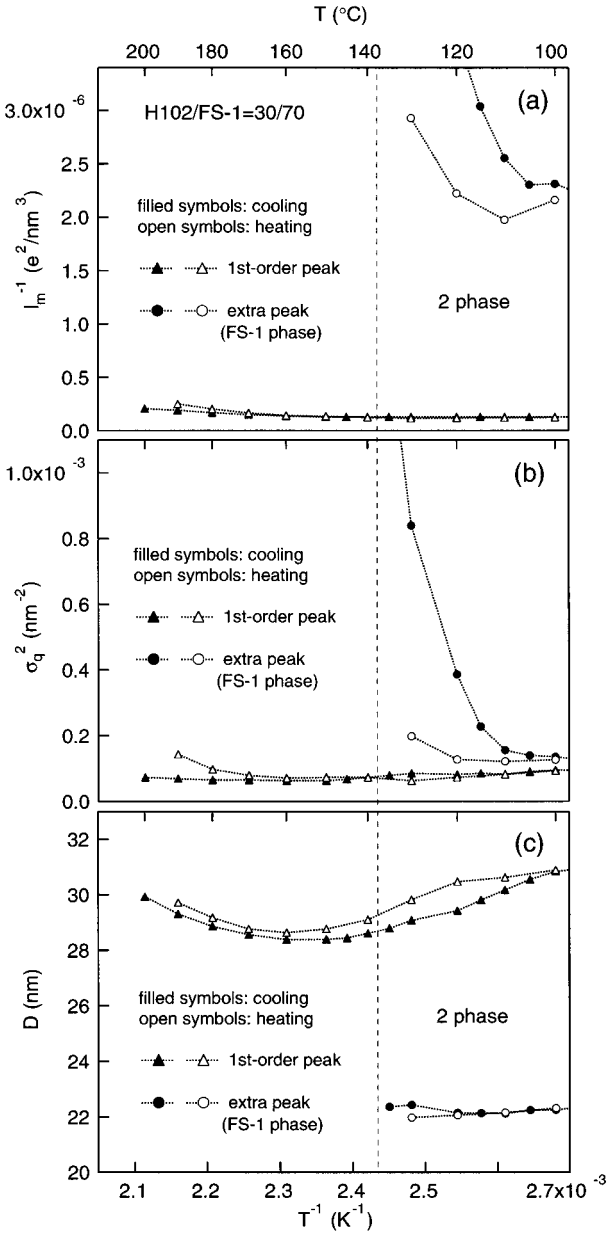

Figure 16. Plots of I_m^{-1} (a), σ_q^2 (b), and D (c) vs T^{-1} for the H102/FS-1 = 30/70 blend. In these plots, the values from the first-order maximum are denoted by triangles (▲, △) and those from the peak marked with an asterisk in Figure 13 which suggests another phase from that corresponds to the first-order peak are denoted by circles (●, ○). And also in these plots, the open and filled symbols denote the values measured on cooling and heating processes, respectively.

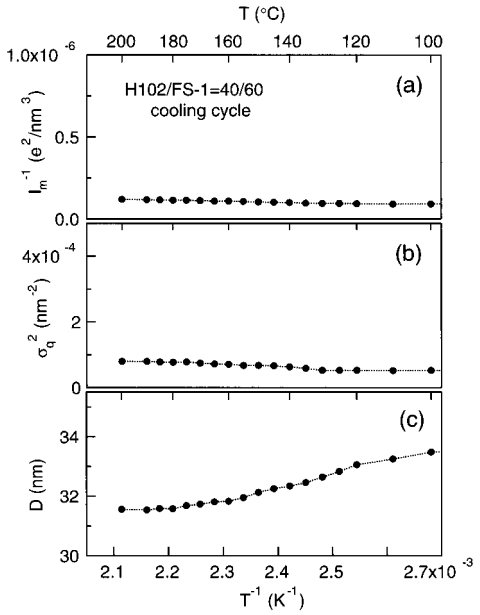

Figure 17. Plots of I_m^{-1} (a), σ_q^2 (b), and D (c) vs T^{-1} for the H102/FS-1 = 40/60 blend. For the 40/60 blend SAXS measurements were conducted only on the cooling process.

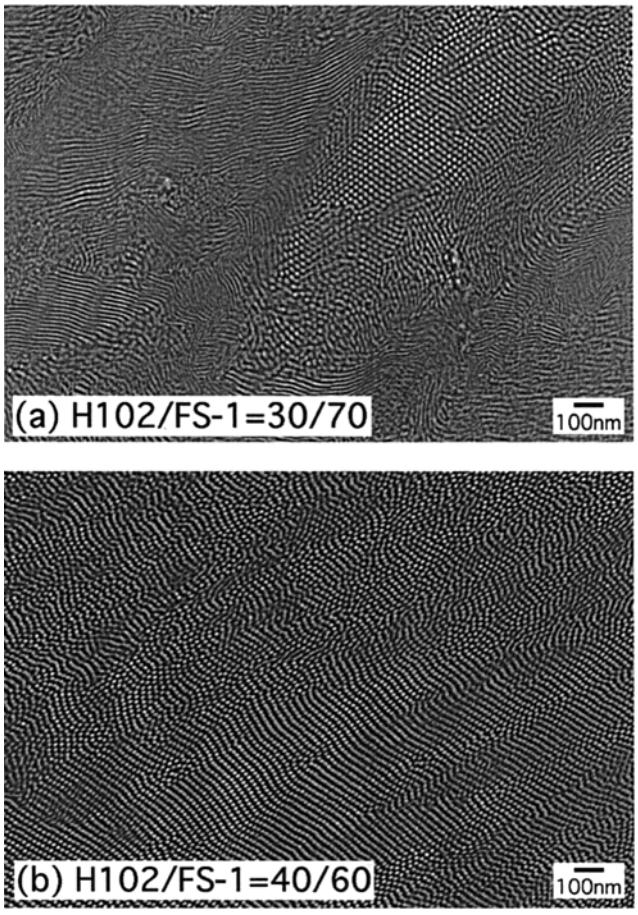

Figure 18. TEM micrographs of H102/FS-1 = 30/70 (a) and 40/60 (b) blends.

of Φ_{H102} destabilizes the lamellar packing and induces the morphological transformation into the hexagonal cylinders with a sharp increase of T_{ODT} with Φ_{H102}. The increase of T_{ODT} with Φ_{H102} which is anticipated to be seen after the morphological transformation from lamellae to hexagonal cylinders may well correspond to the

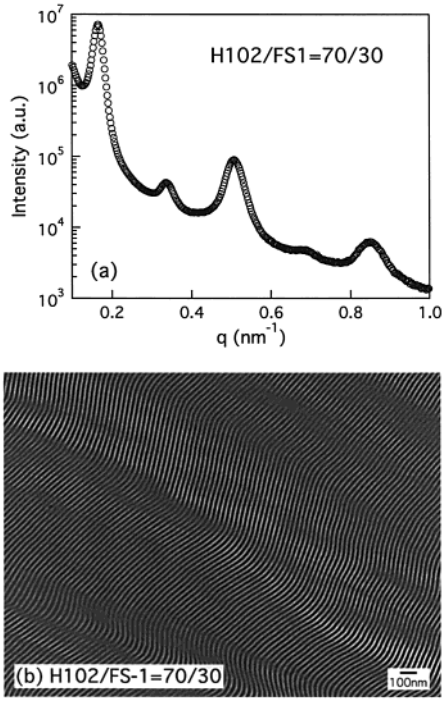

Figure 19. Smeared SAXS profile (a) and TEM micrograph (b) of the H102/FS-1 = 70/30 blend.

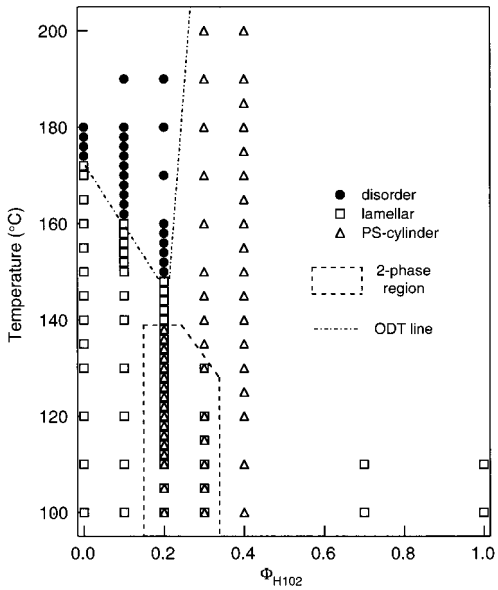

Figure 20. Phase diagram for the H102/FS-1 blend system. Morphology map for all the specimens is presented in the parameter space of temperature and Φ_{H102}. In this map, filled circle (●), open square (□), and open triangle (△) denote disordered state, lamella, and PS cylinder, respectively.

previously reported results by Almdal et al.[12] and Floudas et al.[18] This point is worthy to be studied in future.

IV.3. Immiscibility between the Constituent Copolymers. In this section we will discuss about the propriety of the macrophase-separated structures, which were experimentally observed on the 20/80 and 30/70 blends, by comparing with the theoretical prediction.[8] As mentioned above in section I, three experimental studies[13,23,27] and one theoretical study[8] are in good agreement on the point that the two compositionally symmetric diblock copolymers with different molecular weights become immiscible, when r exceeds about 5,

while r of H102 to FS-1 is 4.8, and this value seems to be quite exquisite to examine the macrophase separation of constituent copolymers induced by temperature change. On the other hand, the macrophase separation of two symmetric diblock copolymers with different polymerization indices was explored by Matsen based on the self-consistent-field theory (SCFT) by varying the segregation power, χN_i.[8] Note here, χ and N_i (i = l or s) denote the Flory−Huggins parameter and polymerization index of long (N_l) or short (N_s) copolymer, respectively. Let us compare the experimental results of H102/FS-1 blends with the calculation results of ref 8, although the rigorous comparison is meaningless due to the some differences in the systems treated by the theory and the experiment. Namely, the theory employed symmetric system not only in compositions of constituent copolymers but also in monomer volumes, segment lengths, and so on, whereas in the experiment, both H102 and FS-1 have asymmetries not only in their compositions but also in monomer volume or segment length between PS and PI. Furthermore, the theory ignored the thermal fluctuation effects whose influence is considerable in the weak segregation regime.

In Figure 1a,b of ref 8, two pieces of the phase diagram sliced at constant $\chi N_l = 80$ and 200 are shown in the parameter space of $\alpha \equiv N_s/N_l$ and the volume fraction of small diblock copolymers, ϕ_s,. Note that $\chi N_l = 80$ and 200 correspond to T = 194 and 9 °C, respectively, for H102/FS-1 blends, assuming that the χ-parameter between PS and PI is given by

$$\chi = 71.4/T - 0.0857 \qquad (1)$$

as reported by Rounds,[41] where T is the absolute temperature, and N_l, i.e., the polymerization index of H102, is equal to 1193. Thus, the sliced phase diagram shown in Figure 1a,b of ref 8 is comparable with the high- and low-temperature parts of the experimental phase diagram for H102/FS-1 blends (cf. Figure 20). Comparing Figure 1a with Figure 1b of ref 8, we discern that the two-phase region extend to higher α as χN_l increases from 80 to 200. Namely the critical point, which is denoted by the dot in Figure 1a or Figure 1b of ref 8, locates at $(\alpha, \phi_s) = (0.185, 0.65)$ for $\chi N_l = 80$, while it locates at $(\alpha, \phi_s) = (0.2, 0.7)$ for $\chi N_l = 200$. Therefore, for example, the point of $(\alpha, \phi_s) = (0.19, 0.7)$ locates in the single-phase region (L) for $\chi N_l = 80$ (corresponds to the high temperature), while it locates in the two-phase region (L + L) for $\chi N_l = 200$ (corresponds to the low temperature). Such a behavior is qualitatively consistent with those observed in the 20/80 and 30/70 blends.

IV.4. Hysteresis Accompanying Macrophase Separation. We observed the very interesting hysteresis accompanied by ODT and macrophase separation. In this section, we will discuss this interesting hysteresis phenomenon observed in the 20/80 blend; the corresponding scattering data are shown in parts a−f of Figure 10. This hysteresis could be rationalized as follows by taking thermal fluctuation effects into account. When the specimen of the 20/80 blend is cooled from disordered state (designated as state I), where H102 and FS-1 are totally mixed in disordered state, the ODT occurs between 150 and 148 °C, and the resultant single ordered phase (designated as state II) emerges. However, the thermal fluctuations lower the ODT temperature of this nearly symmetric blend system and change the nature of the ODT from second-order phase transition to first-order phase transition.[42−45] As the temperature is lowered below 140 °C, the state II becomes unstable and turns into macrophase-separated state (designated as state III). Once macrophase separation takes place and the H102-rich and FS-1-rich phases are formed, the magnitude of fluctuation effects is not uniform any longer but relatively small in the H102-rich phase and relatively large in the FS-1-rich phase. Therefore, when the 20/80 blend is heated from state III, disordering of H102-rich and FS-1-rich phases occur one by one at different temperatures. Furthermore, the T_{ODT} of the H102-rich phase (>150 °C) is higher than that of the uniform 20/80 blend (149 ± 1 °C), which is obtained on the cooling process, due to the effectively suppressed thermal fluctuation.[46] Consequently, in the disordering process, state II is never developed. At present the above scenario is just speculative. However, as to the hysteresis behavior of the 20/80 blend itself, we have checked the reproducibility and believe that it is not artificial but natural.

V. Concluding Comments

In this study, we have investigated the phase behavior of the binary blends of polystyrene-*block*-polyisoprene (PS−PI) copolymers in the parameter space of temperature and blend composition for a particular parameter r, defined as the molecular weight ratio of two constituent PS−PI's, equals 4.8. The larger copolymer having $M_n = 1.0 \times 10^5$ and $f_{PS} = 0.47$ was blended with the smaller copolymer having $M_n = 2.1 \times 10^4$ and $f_{PS} = 0.40$, where M_n and f_{PS} denote the number-average molecular weight and the volume fraction of PS, respectively; then the blends showed a variety of phase behaviors including thermoreversible macrophase separation between the larger and smaller copolymers.

At ambient temperature the morphologies of the blends are rational and in agreement with the theory.[4d,8] On the other hand, concerning the order−disorder transition (ODT) and thermoreversible macrophase separation occurred by temperature change, the blend specimens showed unusual behaviors. As for the ODT, the ODT temperature (T_{ODT}) of the blends presented the following tendency: as the weight fraction of larger copolymer in the blend is increased, the T_{ODT} is lowered. This tendency is contrary to the prediction based on the self-consistent mean-field theory.[8] Another interesting behavior is the hysteresis accompanied by the thermoreversible macrophase separation, which was observed on the blend specimen containing 0.2 weight fraction of larger copolymer. This hysteresis behavior is also unusual, and the thermal fluctuation is considered to play a crucial role in these unusual behaviors.

Acknowledgment. We thank Dr. Mikihito Takenaka, Professor Toshihiro Kawakatsu, and Dr. Hiroshi Morita for very useful suggestions and discussions. This work was financially supported in part by a Grant-in-Aid for Scientific Research (under Grant 12305060(A) and Grant 12640392(C)) from the Ministry of Education, Science and Culture, Japan, and by the national project, which has been entrusted to the Japan Chemical Innovation Institute (JCII) by the New Energy and Industrial Technology Development Organization (NEDO) under MITI's Program for the Scientific Technology Development for Industries that Creates New Industries.

References and Notes

(1) Hashimoto, T. In *Thermoplastic Elastomers, A Comprehensive Review*; Legge, N. R., Holden, G., Schroeder, H. E., Eds.; Hanser: Munich, 1996; p 429. Hasegawa, H.; Hashimoto, T. In *Comprehensive Polymer Science, Second Supplement*; Aggarwal, S. L., Russo, S., Vol. Eds.; Pergamon: New York, 1996; p 497.

(2) Bates, F. S.; Fredrickson, G. H. *Annu. Rev. Phys. Chem.* **1990**, *41*, 525.

(3) Milner, S. T.; Witten, T. A.; Cates, M. E. *Macromolecules* **1989**, *22*, 853.

(4) (a) Birshtein, T. M.; Liatskaya, Y. V.; Zhulina, E. B. *Polymer* **1990**, *31*, 2185. (b) Zhulina, E. B.; Birshtein, T. M. *Polymer* **1990**, *32*, 1299. (c) Zhulina, E. B.; Lyatskaya, Y. V.; Birshtein, T. M. *Polymer* **1992**, *33*, 332. (d) Lyatskaya, J. V.; Zhulina, E. B.; Birshtein, T. M. *Polymer* **1992**, *33*, 343. (e) Birshtein, T. M.; Lyatskaya, Y. V.; Zhulina, E. B. *Polymer* **1992**, *33*, 2750.

(5) Shi, A.-C.; Noolandi, J. *Macromolecules* **1994**, *27*, 2936.

(6) Spontak, R. J. *Macromolecules* **1994**, *27*, 6363.

(7) Shi, A.-C.; Noolandi, J. *Macromolecules* **1995**, *28*, 3103.

(8) Matsen, M. W. *J. Chem. Phys.* **1995**, *103*, 3268.

(9) Matsen, M. W.; Bates, F. S. *Macromolecules* **1995**, *28*, 7298.

(10) Hadziioannou, G.; Skoulios, A. *Macromolecules* **1982**, *15*, 267.

(11) Hashimoto, T. *Macromolecules* **1982**, *15*, 1548.

(12) Almdal, K.; Rosedale, J. H.; Bates, F. S. *Macromolecules* **1990**, *23*, 4336.

(13) Hashimoto, T.; Yamasaki, K.; Koizumi, S.; Hasegawa, H. *Macromolecules* **1993**, *26*, 2895.

(14) Hashimoto, T.; Koizumi, S.; Hasegawa, H. *Macromolecules* **1994**, *27*, 1562.

(15) Koizumi, S.; Hasegawa, H.; Hashimoto, T. *Macromolecules* **1994**, *27*, 4371.

(16) Vilesov, A. D.; Floudas, G.; Pakula, T.; Melenevskaya, E. Y.; Birshtein, T. M.; Lyatskaya, Y. V. *Macromol. Chem. Phys.* **1994**, *195*, 2317.

(17) Bodycomb, J.; Yamaguchi, D.; Hashimoto, T. *Polym. J.* **1996**, *28*, 821.

(18) Floudas, G.; Vlassopoulos, D.; Pitsikalis, M.; Hadjichristidis, N.; Stamm, M. *J. Chem. Phys.* **1996**, *104*, 2083.

(19) Court, F. These de Doctorat de l'Université Pierre et Marie Curie, 1996.

(20) Zhao, J.; Majumdar, B.; Schulz, M. F.; Bates, F. S.; Almdal, K.; Mortensen, K.; Hajduk, D. A.; Gruner, S. M. *Macromolecules* **1996**, *29*, 1204.

(21) Spontak, R. J.; Fung, J. C.; Braunfeld, M. B.; Sedat, J. W.; Agard, D. A.; Kane, L.; Smith, S. D.; Satkowski, M. M.; Ashraf, A.; Hajduk, D. A.; Gruner, S. M. *Macromolecules* **1996**, *29*, 4494.

(22) Lin, E. K.; Gast, A. P.; Shi, A.-C.; Noolandi, J.; Smith, S. D. *Macromolecules* **1996**, *29*, 5920.

(23) Kane, L.; Satkowski, M. M.; Smith, S. D.; Spontak, R. J. *Macromolecules* **1996**, *29*, 8862.

(24) Yamaguchi, D.; Hashimoto, T.; Han, C. D.; Baek, D. M.; Kim, J. K.; Shi, A.-C. *Macromolecules* **1997**, *30*, 5832.

(25) Sakurai, S.; Umeda, H.; Yoshida, A.; Nomura, S. *Macromolecules* **1997**, *30*, 7614.

(26) Sakurai, S.; Irie, H.; Umeda, H.; Nomura, S.; Lee, H. H.; Kim, J. K. *Macromolecules* **1998**, *31*, 336.

(27) Papadakis, C. M.; Mortensen, K.; Posselt, D. *Eur. Phys. J. B* **1998**, *4*, 325.

(28) Koneripalli, N.; Levicky, R.; Bates, F. S.; Matsen, M. W.; Satija, S. K.; Ankner, J.; Kaiser, H. *Macromolecules* **1998**, *31*, 3498.

(29) Yamaguchi, D.; Bodycomb, J.; Koizumi, S.; Hashimoto, T. *Macromolecules* **1999**, *32*, 5844.

(30) Yamaguchi, D.; Takenaka, M.; Hasegawa, H.; Hashimoto, T. *Macromolecules* **2001**, *34*, 1707.

(31) Yamaguchi, D.; Hashimoto, T. *Macromolecules* **2001**, *34*, 6495.

(32) (a) Koizumi, S.; Hasegawa, H.; Hashimoto, T. *Macromolecules* **1994**, *27*, 6532. (b) Koizumi, S.; Hasegawa, H.; Hashimoto, T. *Macromolecules* **1994**, *27*, 7893.

(33) Hashimoto, T.; Suehiro, S.; Shibayama, M.; Saijo, K.; Kawai, H. *Polym. J.* **1981**, *13*, 501.

(34) Suehiro, S.; Saijo, K.; Ohta, Y.; Hashimoto, T. *Anal. Chim. Acta* **1986**, *189*, 41.

(35) Fujimura, M.; Hashimoto, T.; Kawai, H. *Mem. Fac. Eng., Kyoto Univ.* **1981**, *43* (2), 224.

(36) Hendricks, R. W. *J. Appl. Crystallogr.* **1972**, *5*, 315.

(37) Kato, K. *J. Polym. Sci., Polym. Lett. Ed.* **1996**, *4*, 35.

(38) It should be noted that the desmearing process causes a substantial change in relative peak intensity of the first-order peak and the second-order peak. For example, in the smeared profile at 130 °C in Figure 10c,d in state III for both the cooling and heating processes, the first-order peak is higher than the second-order peak. However, this trend is reversed after desmearing as seen in the corresponding profile in Figure 9 and intensity in Figure 12. Note furthermore that in Figure 10 we have shown the smeared SAXS profiles to avoid any "artifacts" which might be caused by the desmearing process. The smeared SAXS profiles were good enough for a qualitative investigation of the change in the scattering behavior accompanied by the change in the self-assembled structures with temperature. Here the "artifacts" mean the extra small peaks or shoulders which might appear on both edges of a main sharp peak caused by dumping oscillation (or instability) in the desmearing process. These artifacts may sometimes mislead the interpretation of the scattering profile. Therefore to avoid the artifacts, we have used the smeared profiles such as shown in Figure 10 for a qualitative investigation of the SAXS profiles. However, for the quantitative estimation of peak intensity (I_m) or peak width (σ_q), the original smeared data are not good enough, and hence we have used the desmeared scattering profiles.

(39) Sakamoto, N.; Hashimoto, T. *Macromolecules* **1998**, *31*, 3815.

(40) It should be noted that in Figure 13b the thickness of lamellar microdomains in different grains appears to be slightly different than each other; namely, the lamellar microdomains located on the left side of the figure are a little thicker than those located on the right side of the figure. This difference may possibly be attributed to the macrophase separation between H102 and FS-1. However, when we checked the quenched specimen by SAXS, we detected only a single first-order peak like the SAXS profile of 145 °C shown in Figure 9a. Therefore, the difference in the thickness of microdomains in Figure 13b may be caused by the artifacts accompanying ultrathin sectioning such as the deformation of the microdomains or by the artifacts due to a different orientation of lamellae in these grains with respect to ultrathin sections.

(41) Rounds, N. A. Ph.D. Dissertation, University of Akron, 1970. It should be noted that there are many studies on the estimation of χ parameter between PS and PI based on PS−PI copolymers. However, in these studies, the measured temperature range is relatively narrower than that of Rounds. Moreover, in these studies the temperature-independent term of χ, namely A, in $\chi = A + B/T$, is sensitive to the molecular weight of using PS−PI copolymers. Therefore, in this study we will use the equation obtained by Rounds. However the conclusion drawn here will not be essentially affected much, at least qualitatively, by the choice of χ.

(42) Brazovskii, A. *Sov. Phys. JETP* **1975**, *41*, 85.

(43) Fredrickson, G. H.; Helfand, E. *J. Chem. Phys.* **1987**, *87*, 697.

(44) Fredrickson, G. H.; Binder, K. *J. Chem. Phys.* **1989**, *91*, 7265.

(45) Sakamoto, N.; Hashimoto, T. *Macromolecules* **1995**, *28*, 6825.

(46) Note that although an unequivocal determination of the ordered state of H102-rich phase at 150 °C on the heating cycle is difficult from the SAXS profile shown in Figure 10f alone, a TEM image obtained for the specimen quenched from 150 °C showed the evidence of some ordered bicontinuous phase (data are not presented in this paper). Therefore, during the heating cycle the H102-rich phase seems to have an order−order transition from PS cylindrical morphology in a low-temperature region (∼100 °C) to some kind of bicontinuous morphology in a high-temperature region around 150 °C, although the transition temperature (T_{OOT}) could not be clearly identified in this work.

MA0021491